Journal of Power Sources 267 (2014) 576–583

Contents lists available at ScienceDirect

Journal of Power Sources

journal homepage: www.elsevier.com/locate/jpowsour

Short communication

Online state-of-health estimation of lithium-ion batteries using Dynamic Bayesian Networks

Zhiwei He, Mingyu Gao*, Guojin Ma, Yuanyuan Liu, Sanxin Chen

Department of Electronic & Information, Hangzhou Dianzi University, 2nd Street, Xiasha Higher Education Zone, Hangzhou 310018, China

HIGHLIGHTS

- A novel SOH estimation method based on Dynamic Bayesian Networks is proposed.
- The SOH can be estimated in an online manner.
- Only terminal voltages during the constant charge process should be measured.
- The estimated SOH can be provided inherently as either a fuzzy or an exact value.

ARTICLE INFO

Article history:
Received 10 December 2013
Received in revised form
8 May 2014
Accepted 21 May 2014
Available online 3 June 2014

Keywords:
Lithium-ion battery
Battery management system
State of health
Dynamic Bayesian Network

ABSTRACT

Li-ion batteries are widely used in energy storage systems, electric vehicles, communication systems, etc. The State of Health (SOH) of batteries is of great importance to the safety of these systems. This paper presents a novel online method for the estimation of the SOH of Lithium (Li)-ion batteries based on Dynamic Bayesian Networks (DBNs). The structure of the DBN model is built according to the experience of experts, with the state of charges used as hidden states and the terminal voltages used as observations in the DBN. Parameters of the DBN model are learned based on training data collected through Li-ion battery aging experiments. A forward algorithm is applied for the inference of the DBN model in order to estimate the SOH in real-time. Experimental results show that the proposed method is effective and efficient in estimating the SOH of Li-ion batteries.

1. Introduction

With the advantages of high cell voltage, low mass, low self-discharge and long cycle life, Li-ion batteries are widely used in energy storage systems, electric vehicles (EVs), communication systems, etc. Energy storage is an enabling technology for power system integration, as it can supply more flexibility for peak shaving and load balancing to the grid, providing a backup to intermittent renewable energy. An energy storage system is also the key component of distributed power systems or smart-grids. In energy storage systems, Li-ion batteries can provide mobile and highly flexible storage capacity and can be placed at several different locations of the grid to ensure efficiency. EVs have numerous advantages over internal combustion engine vehicles in terms of operational convenience, cleanliness, and energy efficiency, and Li-ion batteries are used as main power sources for them. In communication systems, Li-ion batteries are used as secondary power sources. The battery states, such as the state of charge (SOC) and the state of health (SOH), are very important to the safety of these systems [1]. The SOC depicts the remaining capacity that can be drawn from a battery, while the SOH is a measure of the battery's ability to store and deliver electrical energy. The SOC reflects the short-term state of a battery, while the SOH depicts the long-term state of a battery. To maintain optimal battery performance and maximize lifespan of a battery unit, a battery management system (BMS) is often used and is of great essence and significance [2,3]. Currently, many SOC estimation methods have been proposed in the literature, and a subset of them have been used in BMS implementations successfully [4,5]. However, there is still much work that needs to be done for the estimation of SOH.

SOH is defined as the ratio of the current maximum capacity of a battery to its nominal capacity as follows:

$$\mathrm{SOH} = Q_{\mathrm{cmax}}/Q_n \times 100\% \quad (1)$$

where Q_{cmax} denotes the current maximum capacity and Q_n refers to the nominal capacity of the battery.

* Corresponding author.
E-mail addresses: zwhe@hdu.edu.cn (Z. He), mackgao@hdu.edu.cn (M. Gao).

http://dx.doi.org/10.1016/j.jpowsour.2014.05.100
0378-7753/

So far, the most reliable means to determine SOH is through off-line discharge testing of batteries [6]. However, off-line testing is time-consuming and usually requires specialized equipment.

Alternately, the internal resistance of a battery increases continuously, along with the digression of the maximum capacity, during its aging process [7]. A SOH estimation method based on the internal resistance estimation was proposed in Ref. [8]. There are two important issues to address for this and similar methods. One issue is that the measurement of battery internal resistance is difficult, and the other is that the relationship between the internal resistance and the SOH is ambiguous. Many studies have been performed relating to these two aspects, respectively. The most common method to measure the internal resistance is the AC impedance method. For example, the authors in Refs. [9] and [10] presented a fast estimation algorithm that models the battery and then estimates the internal resistance using the Extended Kalman Filter (EKF). To address the relationship between resistance and SOH, the authors in Ref. [11] redefined SOH as a function of resistances. However, this new SOH prediction concept still needs to gain widespread recognition. Another popular method of SOH estimation is to combine the internal resistance with fuzzy logic [12]. However, the battery internal resistance is not only related to the SOH but also the SOC. In other words, the battery internal resistance will rise with the reduction of SOC. Therefore, there is still much left to be done before the internal resistance can be used to estimate SOH precisely.

Efficient calculation and real-time computing are the development trends for SOH estimation. Recently, researchers proposed various data-driven methods for battery SOH estimation [13–16]. In Ref. [13], the authors utilized the famous machine learning algorithm, support vector machine, to estimate the SOH by using load collectives as the training and test data. The authors in Ref. [14] first developed an empirical model based on the physical degradation behavior of lithium-ion batteries, with the model parameters initialized by combining sets of training data based on Dempster–Shafer theory. The Bayesian Monte Carlo is then used to predict the remaining useful life based on available data from battery capacity monitoring. In Ref. [15], the authors utilized a probability neural network to estimate the battery SOH, with three significant characteristics as the inputs. The three used characteristics are the length of the constant current charge time, the voltage drop during the alternation of the constant voltage charge and the constant current discharge, and the initial voltage at the constant current charge. Similarly, the authors in Ref. [16] utilized four characteristics, capacity, resistance, length of the constant current charge time and length of the constant voltage charge time, to estimate the SOH. The key to these data-driven methods is two-fold. The first is what kind of characteristics are to be used for SOH estimation. The second is how to combine these characteristics with a proper inference algorithm. In this paper, we also propose a data-driven method for estimating the SOH of Li-ion batteries. The proposed novel method is based on Dynamic Bayesian Networks (DBNs). In this method, consecutive terminal voltages of batteries during constant charge processes are recorded as training data. The training data are first categorized into K different classes according to the SOH of batteries, and K corresponding DBNs are built. The structure of each model is the same and is built according to the experience of experts, while the parameters of the models are different and are learned based on each category of training data. A forward algorithm is then applied to real-time data of batteries for the inference of the DBN models, to estimate the SOH in real-time.

The main contributions of the paper are as follows: Firstly, a novel DBN-based method is proposed to estimate the SOH for Li-ion batteries. Although DBN has been widely used in many application fields, to our knowledge, it has never been used for SOH estimation. Secondly, the proposed method is an online estimation method, and only terminal voltages during the constant charge process should be measured. Thirdly, the final estimated SOH can be provided as either a fuzzy value or an exact value.

The rest of this paper is organized as follows: Section 2 describes, in detail, the battery aging procedures, which provide the data acquired for training DBNs. Section 3 focuses on the proposed DBN-based SOH estimation method. Section 4 shows a forward algorithm that can be used to estimate the SOH in real time. To validate the SOH prediction method presented, an experiment is conducted and the results are presented in Section 5. Finally, Section 6 states the main conclusion of this paper.

2. Life-cycle testing of batteries

In this research, Li–Mn batteries are used for the life-cycle test, which is performed in a laboratory. Detailed electrical characteristics of the batteries are shown in Table 1. Fig. 1 illustrates the experimental equipment used for the life-cycle testing.

As shown in Fig. 1, batteries are discharged by the programmable electronic load IT8513B, manufactured by ITECH Electronics Co. Ltd., and charged by the power supply JC6030A, manufactured by Hangzhou Jingce Electronic Co. Ltd. A multi-meter UT804, manufactured by Uni-Trend Group Limited, connected to a PC is used to measure and store the voltages of the battery. In the meantime, the internal resistance of the battery is measured by a battery HiTester BT3562-01, manufactured by Hioki.

An initial capacity test was first conducted. The test was initiated by discharging the battery to 0% SOC at a current rate of 1 C. The capacity test then continued by charging the battery to 100% SOC, letting it rest for two hours, discharging it back to 0% SOC, and letting it again rest for two hours; this process constituted one capacity measurement. This initial capacity measurement was repeated several times until the two most recent values of capacity converged to be within an acceptable percentage of one another. This initial capacity test serves to recondition the battery [17].

A complete life cycle test is composed of a charge process and a discharge process. First, the battery was fully charged. The charge process usually consists of two parts: the constant current (CC) subinterval and the constant voltage (CV) subinterval, as shown in Fig. 2. A current of 2.4 A (0.4 C) was used to charge the battery during the CC subinterval until the battery reached its cutoff voltage (4.2 V). Then, the voltage was held constant at 4.2 V during the CV subinterval until the current fell to 100 mA. In the process of charging, the voltages of the battery were measured and stored every 10 s. Secondly, the battery is rested to restore stability. Next, a constant current of 6 A (1 C) was used to discharge the battery, and the cutoff voltage was set to 2.75 V. During the discharge process, the currents and time stamps were recorded to calculate the current maximum capacity, Q_{cmax}, of the battery. During the life-cycle testing, the batteries are placed in a constant temperature chamber at 25 °C.

Table 1
Electrical characteristics of the batteries.

Typ. voltage	3.7 V
Nominal capacity	6000 mAh, 1 C discharge
Maximum charge current	1 C
Maximum discharge current	1 C
Minimum discharge voltage	2.75 V
Maximum charge voltage	4.2 V
Discharge temperature	−20 °C to 60 °C
Initial internal impedance	≤20 mΩ
Self-discharge current	≤200 μA
Cycle life (minimum)	800 cycles

Fig. 1. Experimental equipment.

$$Q_{cmax} = \int_{t1}^{t2} I(t)dt \tag{2}$$

The actual SOH of a battery can be calculated with Formula (1).

The life cycle testing was repeated several times until the capacity degraded to 80% of its nominal capacity, and the collected data were then used to train the DBN model.

3. DBN for SOH estimation

3.1. General introduction of DBN

A Bayesian Network (BN) represent a set of variables in the form of nodes on a directed acyclic graph. It maps the conditional independencies of these variables. A DBN is a BN extended with a temporal dimension to enable us to model dynamic systems.

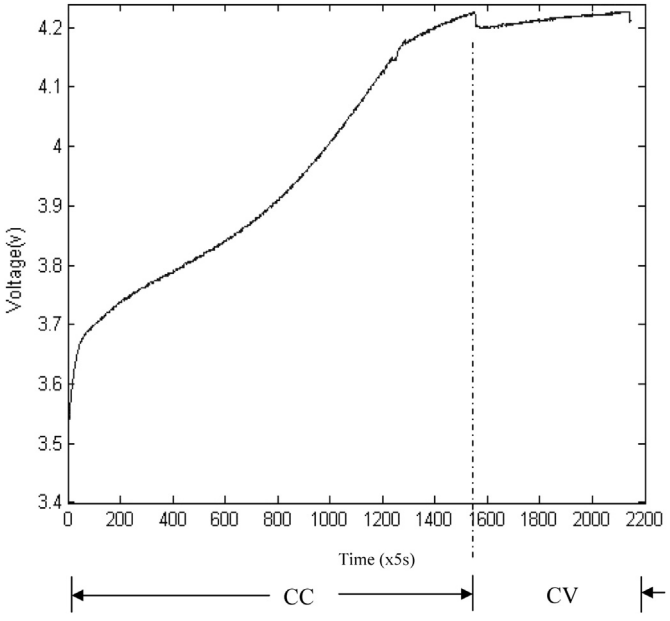

Fig. 2. Charge process of batteries.

A DBN is defined as a pair $(B_0,B_{\rightarrow})$, where B_0 defines the prior $P(Z_1)$ and $B_{\rightarrow}$ is a two-slice temporal Bayes net that defines $P(Z_t|Z_{t-1})$ by means of a directed acyclic graph as follows:

$$P(Z_t|Z_{t-1}) = \prod_{i=1}^{N} P\left(Z_t^i \middle| p_a\left(Z_t^i\right)\right) \tag{3}$$

where Z_t^i is a node at time slice t, which can be a hidden node, an observation node or a control node; and $p_a(Z_t^i)$ are parent nodes of Z_t^i, which can be at either time slice t or $t-1$. To specify a DBN, one must define its structure, i.e., the intra-slice topology and the inter-slice topology, as well as the parameters for the first two slices (the conditional probability distributions).

DBNs are common in robotics and have shown potential for a wide range of applications. For example, they have been used in speech recognition, digital forensics, protein sequencing, bioinformatics, etc. As aforementioned, a DBN is applied for the battery SOH estimation in this paper.

3.2. The DBN model for SOH estimation

Although the SOC and the SOH are two distinct states of a battery, they are related to each other, for instance, by the internal resistance. Many methods utilize the same battery circuit model to estimate the SOC and the SOH simultaneously. Batteries with different SOHs will have different SOC–OCV (open circuit voltage) curves. In this research, the structure of the DBN is created as shown in Fig. 3.

In Fig. 3, the SOCs are the hidden nodes of the DBN model, which cannot be observed directly. Terminal voltages of the battery are chosen as the observed nodes of the DBN. $\pi = (\pi_i)$ denotes the vector of the initial state probabilities, defining the probability of the system being in each of the states at the initial time. $A = (a_{ij})$ is the state transition matrix, which defines the transition probability of the SOC at time t given the previous SOC at time $t-1$, i.e., $a_{ij} = P(\mathrm{SOC}_i^t | \mathrm{SOC}_j^{t-1})$. $B = (b_{ij})$ refers to the confusion matrix, which contains the probabilities of the observed voltages given the hidden state SOC, i.e., $b_{ij} = P(V^t = V_i | \mathrm{SOC}^t = S_j)$ [18].

As mentioned before, the DBN model is built only for the CC subinterval of the charge process in Fig. 2.

3.3. Parameter learning

The parameters for the DBN model are $\pi = (\pi_i)$, $A = (a_{ij})$ and $B = (b_{ij})$.

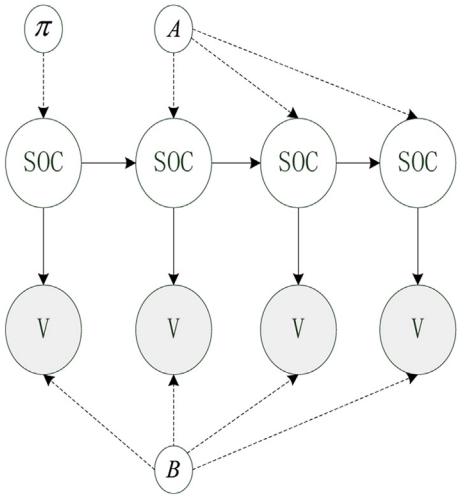

Fig. 3. The structure of the DBN.

In the original DBN model, the observed and hidden nodes can be either discrete or continuous. For simplification, in this research the SOCs and the terminal voltages are discretized before parameter learning.

Because the DBN is built in the CC subinterval of the charge process, we consider only the SOCs in this interval. The SOC state where the terminal voltage reaches its maximum value during the CC subinterval is defined as a full SOC. Then, the SOC range between 0% and the full state is divided into N equal subsections, and the i-th class S_i has a SOC range in between $100\% \times (i-1)/N$ and $100\% \times i/N$, as shown in Table 2 ($N = 30$ in this table).

The terminal voltages in the CC mode are also classified into M classes, with the j-th class having a voltage range in between $V_{\min} + (V_{\max} - V_{\min}) \times (j-1)/M$ and $V_{\min} + (V_{\max} - V_{\min}) \times j/M$, where $V_{\min}$ is the minimum terminal voltage in the charge process and $V_{\max}$ is the maximum voltage; for the batteries used in this research, $V_{\min} = 3.6$ V and $V_{\max} = 4.2$ V.

In the beginning, the SOC may be in any condition, so the initial state of SOC is regarded as uniformly distributed. Thus, we have

$$P\left(\mathrm{SOC}^0 = S_i\right) = 1/N (i = 1, 2, \cdots, N) \tag{3a}$$

According to the definition of π_i we have

$$\pi_i = P\left(\mathrm{SOC}^0 = S_i\right) \tag{4}$$

The size of matrix $A = (a_{ij})$ and matrix $B = (b_{ij})$ are $N \times N$ and $M \times N$, respectively, and they can be calculated according to the Bayes' rule:

$$a_{ij} = P\left(\mathrm{SOC}^t = S_i \middle| \mathrm{SOC}^{t-1} = S_j\right) = \frac{P(\mathrm{SOC}^t = S_i, \mathrm{SOC}^{t-1} = S_j)}{P(\mathrm{SOC}^{t-1} = S_j)} = \frac{\#(\mathrm{SOC}^t = S_i, \mathrm{SOC}^{t-1} = S_j)}{\#(\mathrm{SOC}^{t-1} = S_j)} \tag{5}$$

$$b_{ij} = P(V^t = V_i | \mathrm{SOC}^t = S_j) = \frac{P(V^t = V_i, \mathrm{SOC}^t = S_j)}{P(\mathrm{SOC}^t = \mathrm{SOC}_j)} = \frac{\#(V^t = V_i, \mathrm{SOC}^t = S_j)}{\#(\mathrm{SOC}^t = S_j)} \tag{6}$$

where $\#(X = x)$ refers to the number of samples that satisfy$X = x$.

The obtained battery charging data are classified into K different classes according to their aging states. The class label k is determined by the value Q_{cmax}/Q_n as follows:

$$\text{if} \quad Q_{\mathrm{cmax}}/Q_n < 80\%, k = K \tag{7}$$

$$\text{if} \quad Q_{\mathrm{cmax}}/Q_n \geq 80\%, k = \left\lfloor \frac{100\% - Q_{\mathrm{cmax}}/Q_n}{20\%/K} \right\rfloor \tag{8}$$

where $\lfloor x \rfloor$ is the minimum integer larger than x. An example of categorization of the aging states into 5 classes is shown in Table 3.

Table 2
Mapping of the real SOC to its label ($N = 30$ in this table).

SOC	0–3.33%	3.33–6.66%	6.66–10%	10–13.33%	13.33–16.66%
Label	1	2	3	4	5
…					
SOC	83.33–86.66%	86.66–90%	90–93.33%	93.33–96.66%	96.66–100%
Label	26	27	28	29	30

Table 3
Categorization of the aging states of a battery (5 classes are used in this example).

Q_{cmax}/Q_n	>95%	95%–90%	90%–85%	85%–80%	<80%
Aging state	Brand-new	New	Ok	Old	Very old
Class label	1	2	3	4	5

A fuzzy representation of the original precise SOHs is defined according to the aging states of batteries, and K different DBNs ($DBN_i, i = 1,2,\ldots,K$) can then be built and trained, respectively, to obtain the fuzzy SOH of a battery.

4. Estimating SOH in real-time

4.1. Forward algorithm

After the structure and parameters of these DBNs are determined, the SOH of batteries can then be estimated. When a battery is charged in a CC mode, the terminal voltages are measured every 30 s T^*30 seconds later, an observed voltage sequence (V_{k1},V_{k2},…, V_{kT}) can be obtained. $P_i(V^{(k)}|DBN_i)$, the probability of the sequence given the DBN, is calculated to distinguish which DBN the sequence belongs to.

As shown in Fig. 4, the observations and the possible hidden states can be pictured as a trellis. One method of calculating $P_i(V^{(k)}|DBN_i)$ is to find the probability of each possible sequence of the hidden states, and take the sum of these probabilities. However, this manner is computationally expensive, and cannot calculate the probability in real-time. To overcome these shortcomings, a forward algorithm is used in this paper, which can calculate the posterior probability recursively to reduce the computational complexity.

The partial probability α, which is the probability of reaching an intermediate state in the trellis, is the key to the forward algorithm.

At time $t = 1$, there are no paths to the initial states, and therefore the partial probabilities at $t = 1$ can be calculated as the initial probability multiplied by the associated observation probability:

$$\alpha_1(j) = \pi_j b_{jk_1} \tag{9}$$

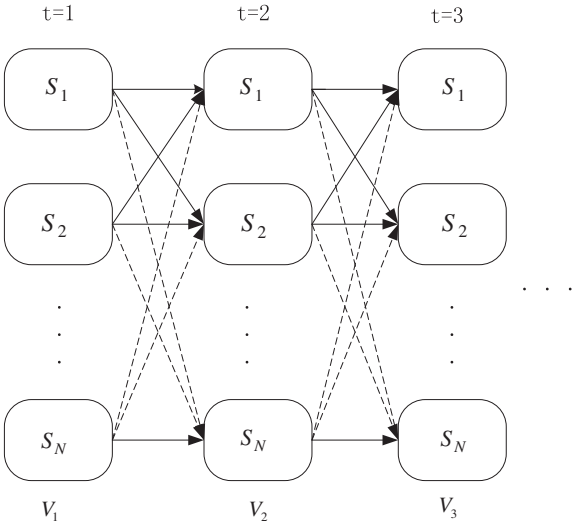

Fig. 4. The trellis showing the states and first-order transitions for the observation sequence.

At times $t = n(n = 2,3,\ldots T)$, because α at time $t = n - 1$ gives the probability of reaching that state through all previous paths, α at time $t = n$ can be calculated as follows:

$$\alpha_{t+1}(j) = \sum_{i=1}^{n} (\alpha_t(i) a_{ij}) b_{jk_i} \tag{10}$$

i.e., the product of the appropriate observation probability and the sum over all possible routes to that state.

Finally, given the DBN_i, the probability of the observation sequence $V^{(k)}$, $P_i(V^{(k)}|DBN_i)$, can be obtained by summing all partial probabilities [19,20]:

$$P_i\left(V^{(k)}\middle|DBN_i\right) = \sum_{j=1}^{n} \alpha_T(j) \tag{11}$$

The computing complex of the forward algorithm is $O(N^{2*}T)$, where N is the number of hidden states and T is the length of the observation sequence.

The flowchart for real-time posterior probabilities calculation is shown in Fig. 5.

4.2. SOH determination

The posterior probabilities are firstly normalized as follows:

$$P_i' = \frac{P_i\left(V^{(k)}|DBN_i\right)}{\sum_{i=1}^{K} P_i(V^{(k)}|DBN_i)} \tag{12}$$

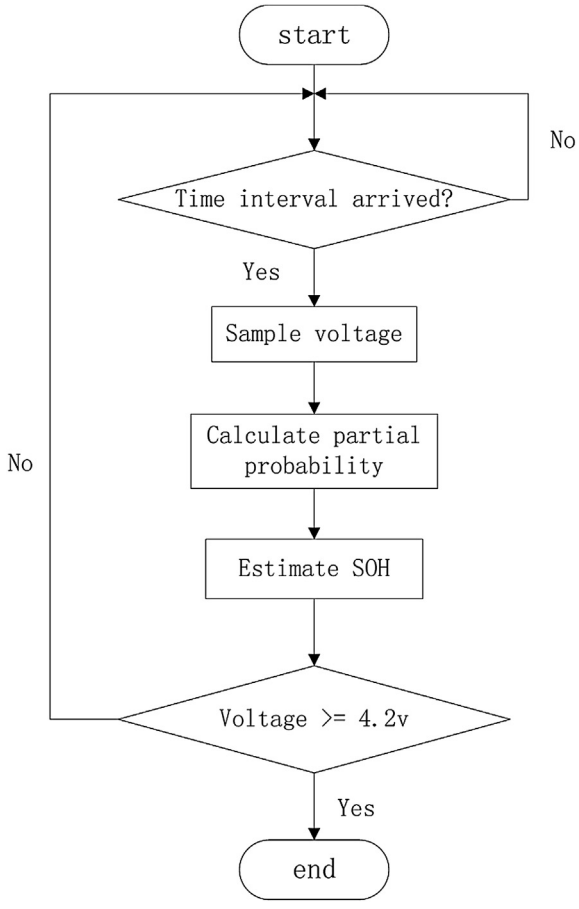

Fig. 5. The flowchart for real-time posterior probabilities calculation.

The corresponding estimated fuzzy SOH is then defined as the aging state of the DBN with a maximum normalized probability.

An estimated exact SOH can also be defined as the sum of the product of the normalized probability of each model with the corresponding lower boundary SOH.

$$SOH_e = \sum_{i=1}^{K} P_i' \left[100\% - i^* \frac{100\% - 80\%}{K - 1}\right] \tag{13}$$

5. Verification

In this research, 21 Li–Mn batteries were used. For each battery, 100 life-cycle tests were performed, and the data were recorded as described in Section 2. To obtain data under different aging conditions, aging accelerating processes were applied randomly to the batteries between some of their life-cycle tests, in which the batteries were discharged under a high temperature of 55 °C. However, all of the charge processes were conducted under a constant room temperature of 25 °C. Among the 21 batteries, 6 were used for model verification only. The 1500 groups of data obtained from the other 15 batteries were mixed together and then divided into two parts: 1400 groups were randomly chosen for model training, and the remaining 100 groups were used for model verification. The training data were firstly divided into 5 categories according to Table 3, resulting in 282, 331, 352, 333 and 102 groups of data, respectively, and five different DBNs were then trained with the data in each of the categories. The voltage profiles used to train the five DBNs are shown in Fig. 6.

The trained DBNs are shown in Fig. 7. In this figure, the first row shows the confusion matrices corresponding to each aging state, from the "brand-new" state to the "very old" state, while the second row shows the corresponding transition matrices. M and N were set to be 60 and 30, respectively, when the DBNs were trained.

The voltage profile of one of the tested life-cycles is shown in Fig. 8. The maximum capacity of this cycle is 5.086 Ah. According to (1), the real SOH of the tested battery, SOH_r, can be obtained as:

$$SOH_r = \frac{5.086}{6} * 100\% = 84.8\% \tag{14}$$

The normalized probabilities obtained from the 5 different DBNs for this voltage profile are shown in Fig. 9. As seen from the figure, the corresponding aging state with the maximum probability is

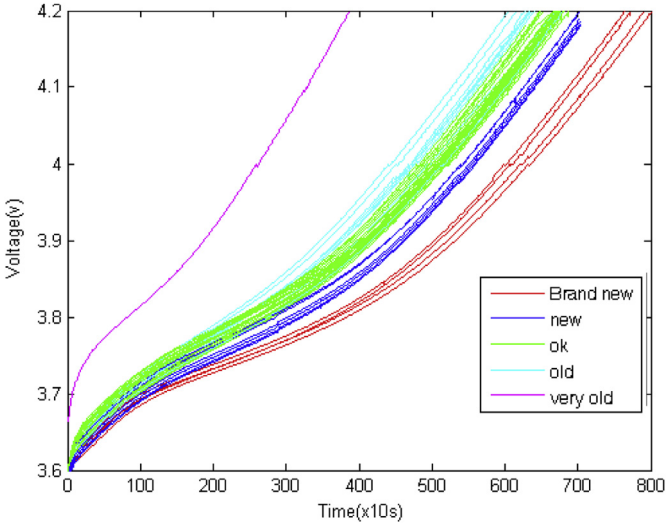

Fig. 6. The voltage profiles used to train the five DBNs.

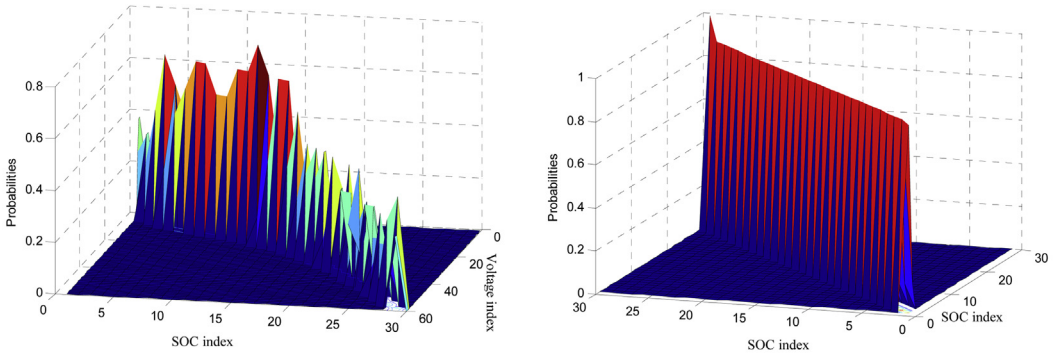

(a) DBN model for the “Brand-new” category

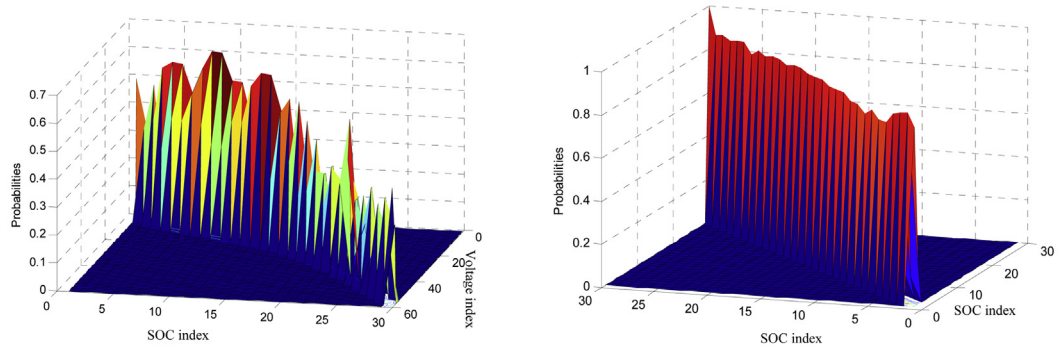

(b) DBN model for the “new” category

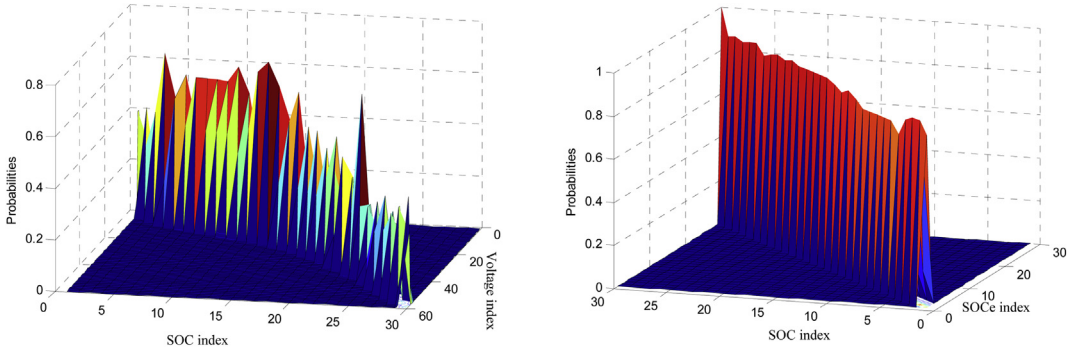

(c) DBN model for the “ok” category

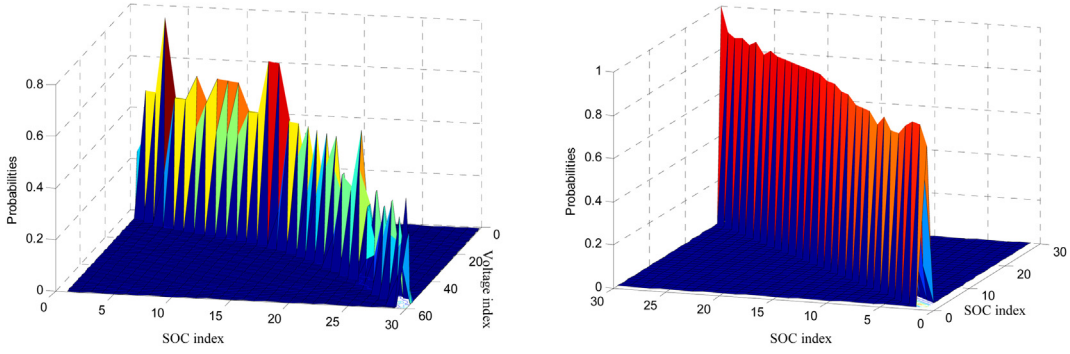

(d) DBN model for the “old” category

Fig. 7. The confusion matrices and transition matrices of the trained DBN models.

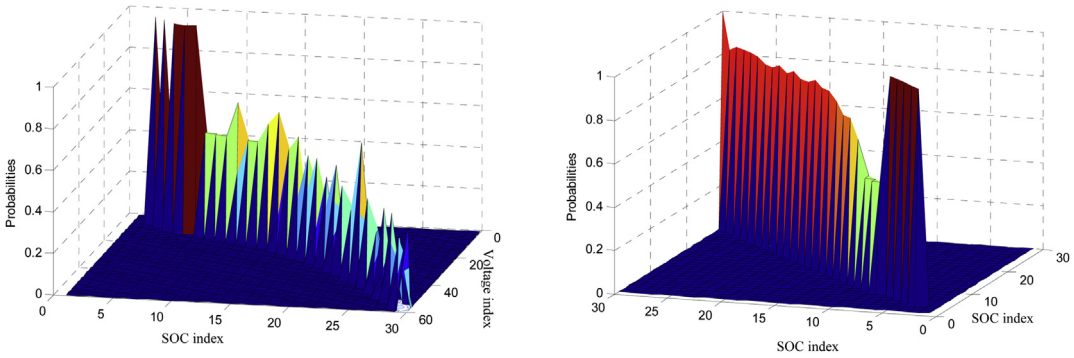

(e) DBN model for the "very old" category

Fig. 7. (*continued*).

"old", whose SOH is in the range between 80% and 85% according to Table 3. We can conclude that the predicted fuzzy SOH is consistent with the real SOH for this cycle. With the normalized probabilities as the weights, we can also obtain the estimated SOH, SOH_e, as a sum of weighted predictions. For the aforementioned example, we can obtain:

$$SOH_e = 0.163*95\% + 0.205*90\% + 0.196*85\% + 0.318*80\% + 0.120*75\% = 85.0\% \quad (15)$$

which is only slightly different than SOH_r.

The other test cycles are also verified with the same process. As a result, 682 groups of data out of the total 700 test cycles are correctly classified, with an estimation error smaller than 3%. The misclassified test cycles mainly come from the "median" category and the "old" category, whose DBN models are similar to each other to some extent, as seen in Fig. 7. For these misclassified test cycles, the absolute error between the estimated SOH and its true value is smaller than 5%.

Furthermore, the proposed method can give an acceptable SOH estimation result even if only part of the terminal voltage profile can be obtained. However, this does not mean that any partial sequence is suitable. Our experiments show that it is better to use at least a considerable portion, if not all, of the charging data in the last part of the CC subinterval (e.g., the part when the terminal voltage goes from 3.8 V to 4.2 V for the tested battery) in order to have good SOH estimation accuracy. For the test cycle in Fig. 8, when only data from 3.8 V to 4.2 V were used, a correct fuzzy SOH estimation result of "old" was still obtained.

6. Conclusions

A novel online SOH estimation method for Li-ion batteries was presented in this paper. Several DBNs have been built and trained according to the aging state of batteries. The SOCs are used as hidden states in the DBNs, while the terminal voltages are used as observations. The training and inference of the DBNs were conducted within the CC mode during a charge process of batteries. The parameters of the models have been learned based on data collected in Li-ion battery life-cycle testing experiments. A forward algorithm was utilized for real-time online estimation of the SOH. Experimental results show that the proposed method is effective for SOH estimation. Only terminal voltages should be measured for the SOH estimation in the proposed method, which is very convenient for real applications. The SOH can be estimated online, and either a fuzzy or an exact estimation result can be given. More DBN models may be needed in order to improve the SOH estimation accuracy, but much more training data will be required. The

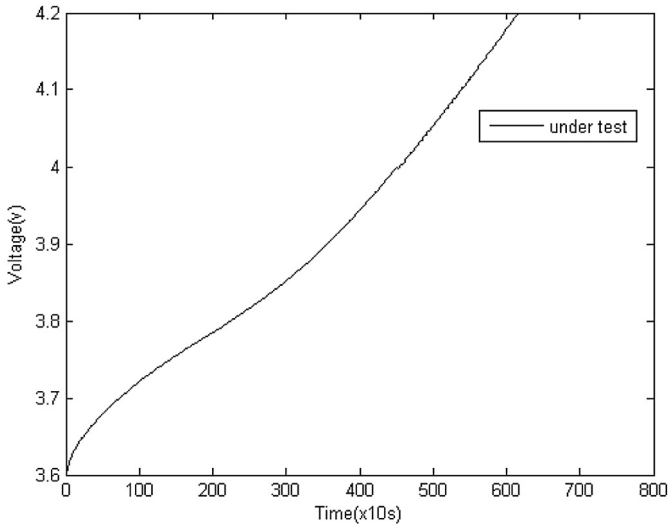

Fig. 8. The voltage profile of a test cycle.

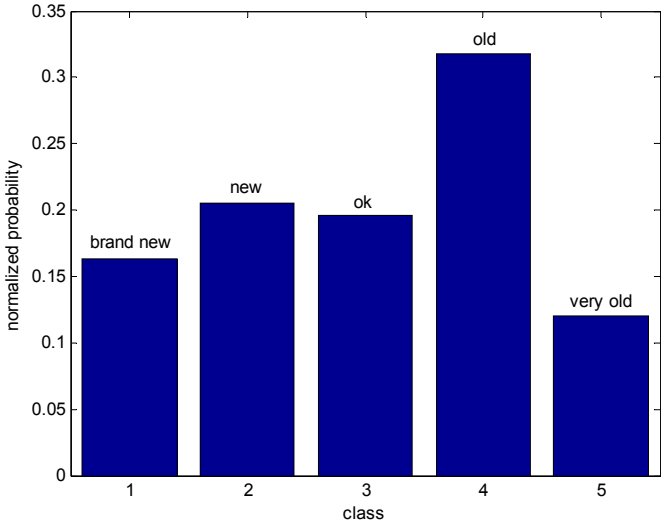

Fig. 9. The nominal probabilities obtained according to the five DBNs.

proposed method can be further improved with more characteristics added as inputs to the DBN models, e.g., the currents in the CV subinterval. Impact of temperature is another problem that should be considered in the future.

Acknowledgment

The authors would like to thank the anonymous reviewers for their insightful comments and suggestions. This work is supported by the National Natural Science Foundation of China (NSFC) Grant #61172132, and Zhejiang Provincial Natural Science Foundation of China Grant #LQ13F010011.

References

[1] Z. Chen, C.C. Mi, Y. Fu, et al., J. Power Sources 240 (10) (2013) 184–192.
[2] J. Kim, S. Lee, et al., J. Power Sources 196 (4) (2011) 2227–2240.
[3] W.L. Chen, J.F. Li, B.X. Huang, Electr. Power Compon. Syst. 39 (15) (2011) 1632–1646.
[4] M. Einhorn, F.V. Conte, et al., IEEE Trans. Ind. Appl. 48 (2) (2012) 736–741.
[5] Z. He, M. Gao, C. Wang, et al., Energies 6 (8) (2013) 4134–4151.
[6] I.L.S. Kim, IEEE Trans. Power Electron. 25 (4) (2010) 1013–1022.
[7] G.K. Prasad, C.D. Rahn, J. Power Sources 232 (6) (2013) 79–85.
[8] Y.H. Chiang, W.Y. Sean, et al., J. Power Sources 196 (8) (2011) 3921–3932.
[9] J. Kim, S. Lee, et al., IEEE Trans. Power Electron. 27 (1) (2012) 436–451.
[10] H. He, R. Xiong, et al., IEEE Trans. Veh. Technol. 60 (4) (2011) 1461–1469.
[11] D. Haifeng, W. Xuezhe, et al., in: Proceeding of IEEE Vehicle Power and Propulsion Conference, Dearborn, USA, 7–10 Sept., 2009.
[12] A. Zenati, P. Desprez, et al., in: Proceeding of IEEE Annual Conference on Industrial Electronics Society, Glendale, USA, 7–10 Nov., 2010.
[13] A. Nuhic, et al., J. Power Sources 239 (2013) 680–688.
[14] W. He, N. Williard, et al., J. Power Sources 196 (23) (2011) 10314–10321.
[15] L. Ho-Ta, L. Tsorng-Juu, C. Shih-Ming, IEEE Trans. Ind. Inform. 9 (2) (2013) 679–685.
[16] N. Williard, W. He, et al., Int. J. Progn. Health Manag. 4 (2013) 1–7.
[17] A.K. Suttman, Lithium Ion Battery Aging Experiments and Algorithm Development for Life Estimation (Master Thesis), The Ohio State University, 2011.
[18] L. Liporace, IEEE Trans. Inf. Theory 28 (5) (1982) 729–734.
[19] B.-H. Juang, S. Levinson, et al., IEEE Trans. Inf. Theory 32 (2) (1986) 307–309.
[20] K.P. Murphy, Dynamic Bayesian Networks: Representation, Inference and Learning (Doctor Thesis), University of California, 2002.